JOURNAL OF CATALYSIS 81, 119–130 (1983)

Electron Microscope Studies of Platinum/Alumina Reforming Catalysts

D. WHITE,* T. BAIRD, AND J. R. FRYER

Chemistry Department, University of Glasgow, Glasgow G12 8QQ, Scotland

AND

L. A. FREEMAN AND DAVID J. SMITH

High Resolution Electron Microscope, University of Cambridge, Free School Lane, Cambridge CB2 3RQ, England

AND

M. DAY

I.C.I. PLC Petrochemicals and Plastics Division, Wilton, Cleveland, England

Received August 2, 1982; revised December 7, 1982

Platinum/alumina catalysts were examined following ageing–regeneration cycles typical of industrial use and after extreme treatments in "oxidising" or "reducing" environments. Details of particle morphology and the statistics of particle size distribution (PSD) were obtained by high-resolution electron microscopy, with complementary data from hydrogen chemisorption measurements. It was found that catalyst sintering during a simulated industrial cycle was minimal, whereas "reducing" or "oxidising" treatments at high temperature (600°C) caused loss of accessible Pt surface area, as measured by chemisorption: the PSDs and particle geometries, however, then differed greatly, despite similar chemisorptive capacities. Conversely, it was also observed that no appreciable particle growth resulted from severe reducing treatment despite a reduced chemisorptive capacity. After 24 days at 600°C the catalyst metal remained as discrete single crystals or twinned Pt particles. No redispersion by oxide spreading was observed after oxidation or "chloriding" treatments; instead, the clustering of Pt metal crystallites to form continuous agglomerates, apparently confined in size and shape only by the three-dimensional geometry of the alumina support, seemed to be commonplace. The irregular morphology of these agglomerates was revealed by stereo-imaging, and hydrogen chemisorption measurements confirmed their high surface areas.

1. INTRODUCTION

There has been renewed interest in the characterisation of supported metal catalysts following heat treatment under various temperatures and atmosphere conditions in order to examine the ageing and reactivation phenomena that occur. Transmission electron microscopy (TEM) is invaluable in these studies since information can be obtained about the size (*1*) and distribution (*2*) of the catalyst particles and, provided sufficient resolution is available (*3*), the detailed chemical composition and structure of both metal (*4*) and support (*5*) may also be identified. Furthermore, many workers have developed model systems, specifically adapted to these ends (*5–8*). However, the relationship between these

* Present address: Analytical Services and Research Division, B.P. Research Centre, Chertsey Road, Sunbury-on-Thames, Middlesex TW16 7LN, England.

0021-9517/83 $3.00

model catalysts and the real ones is qualitative at best (*9*), and there is also a possibility that artefacts will be introduced by the method of preparation (*10*). Comparable studies of the real catalysts are clearly needed. Chemisorption measurements can provide useful complementary data since the metal surface area available for catalysis can be measured. For example, very high surface areas of platinum on alumina have been observed (*11*), and changes in surface area following thermal treatment have been detected (*12, 13*). These changes have been linked to dispersion of the platinum particles although this is only one possible explanation.

The re-dispersion of sintered metal particles has been claimed by various authors and mechanistic details have been proposed. For example, the fracture of large platinum crystallites on model alumina supports into several smaller crystallites was suggested by Ruckenstein and Malhotra (*14*), although similar experiments repeated by Stulga *et al.* (*15*) could not confirm this result. Ruckenstein and Chu (*16*) have described the sintering/re-dispersion behaviour of similar Pt/Al_2O_3 model catalysts after cyclic reduction/oxidation treatments, using 1 atm of H_2 and O_2, respectively, at 750°C; crystallite-fracture and oxide-spreading mechanisms were developed to account for these observations. A similar spreading mechanism was proposed by Baker *et al.* (*5*) which involved the formation of metal layers interacting strongly with the support. However, this was only demonstrated via the Pt-catalysed reduction of TiO_2 to Ti_4O_7 in platinum/titania model catalysts.

The spreading of metal oxides on the support, with regained metal surface area following reduction, has been supported by several studies (*16–18*) with strong evidence being obtained in Rh/SiO_2, Rh/γ-Al_2O_3 (*18*), and Ir/SiO_2 (*19*) systems. Derouane *et al.* (*20*) also observed the spreading of iridium oxide on graphite during direct examination by controlled-atmosphere electron microscopy. However, this effect has not been clearly demonstrated for platinum on alumina, although platinum oxide or oxychloride complexes with alumina have been suggested (*15, 21*). McHenry *et al.* (*21*) were able to detect a platinum/alumina complex in their catalysts, which was termed "soluble" platinum, since it could be dissolved out in hydrofluoric acid or acetylacetone. Similarly, Yao *et al.* (*13*) used temperature-programmed reduction (TPR) to detect "particulate" and "dispersed" phases of Pt oxide on alumina, the latter having a strong interaction with the support, as with the soluble Pt found by McHenry *et al.* (*21*). Conversely, Wang and Schmidt (*18*) detected only Rh re-dispersion around Pt cores in STEM studies of supported Rh/Pt alloy catalysts, whilst Foger and Jaeger (*19*), using TPR, TEM, and X-ray diffraction, found no traces of any platinum oxides after heating Pt/Al_2O_3 catalysts at temperatures of 100–700°C.

This paper reports TEM examinations of Pt/γ-Al_2O_3 catalysts following a pseudoindustrial ageing–regeneration cycle, as well as their characterisation after various "oxidising" and/or "reducing" treatments, with hydrogen chemisorption measurements providing complementary data. The particle morphologies strongly reflected the difference in sintering rates due to the reducing or oxidising environments, in good qualitative agreement with model studies (*4, 8*).

2. EXPERIMENTAL

2.1. Catalyst preparation. A batch of alumina (Condea SB) was mixed with a few millilitres of dilute acetic acid, pelleted, ground, and sieved to 500-μm granules. These granules were then calcined at 600°C in air for 84 hr and cooled to room temperature. Portions of the resultant γ-Al_2O_3 were impregnated with predetermined amounts of hexachloroplatinic acid and dilute HCl to give the desired Pt and Cl loadings, which

were confirmed by neutron activation analysis. Detailed results are reported below for catalyst A, containing 0.4% by weight of Pt, 0.8 w/o Cl, and catalyst B, containing 2.0 w/o Pt, 0.8 w/o Cl.

2.2 Catalyst treatments. Catalyst samples, each weighing 1 or 2 g, were packed into stainless-steel reactor tubes in a laboratory-scale reformer and subjected to various temperature/time/gas flow treatments, as detailed in Tables 1 and 2. The initial treatment before single-step experiments, and prior to cyclic procedures, involved reduction in flowing H_2 at 400°C for 3 hr. A lab-scale reforming cycle was carried out, consisting of a series combination of reduction, ageing, burnoff, and oxychlorination steps. The following conditions were established for catalyst ageing in flowing naphtha:

Reactor temperature:	510°C
Reactor pressure:	200 psig
Naphtha WHSV:	2.5 hr^{-1}
H : HC:	6 : 1

The catalyst was aged for 1 week, and then carbon was removed by controlled burnoff, at 480°C, in flowing 3% by volume of O_2 in N_2 gas mixture, until CO_2 evolution ceased, this taking around 5 hr. Controlled amounts of chlorine were added to burnt-off or presintered catalysts via a stream of CCl_4, injected slowly into the reactor gas flow. This oxychlorination stage was carried out at 480°C, under 2 litres/hr flow of 3 v/o O_2 in N_2, and lasted 2–5 hr, depending on the amount of Cl added. Catalyst portions could be discharged at any stage for characterisation.

2.3. Chemisorption measurements. Catalyst samples were first heated to 400°C and reduced in 200 Torr H_2 over 2½ hr, followed by heating at 400°C and evacuation for 6 hr. An adsorption isotherm was then measured for 120, 160, and 200 Torr H_2 and the volume of H_2 adsorbed at zero pressure was extrapolated and designated the monolayer volume (V_m). The H : Pt chemisorption ratio was taken at 1 : 1. A simple spherical particle geometry was assumed and, on this basis, mean particle diameters expected from chemisorption measurements were calculated ($\bar{d}_{calc}$); these are tabulated with the TEM results.

2.4. Electron microscopy. Specimens were prepared for high-resolution TEM examination by dry-mounting some finely ground catalyst on "holey" carbon support films. Alternatively, ultrasonically dispersed catalyst grindings were dried onto the support film from propan-2-ol. A thin carbon film was often vacuum-deposited onto prepared specimens for additional stability and to minimise charging in the electron beam which was usually a problem at high magnification. Specimens were then examined in a JEOL 100C electron microscope and in the Cambridge University 600-kV high-resolution electron microscope (HREM) (*22, 23*). The capacity for direct lattice imaging in small metal particles of the latter microscope (*24*) was particularly useful for studying the morphology of the supported Pt, although overlapping lattice fringe contrast arising from γ-alumina support was often confusing. Stereo TEM images were also obtained, using specimen tilts, typically of 5°, to reveal further details of the three-dimensional geometry of the catalysts. A standard optical bench, equipped with a 10-mW He–Ne laser, was used for measurement and analysis of the periodicities present in the high-resolution images.

2.5. Statistical analyses. The particle size distributions (PSDs) were obtained from diameter measurements of up to 500 particles per catalyst sample with large particles being measured directly from TEM negatives and small particles from photographic print enlargements. For irregularly shaped particles the longest and shortest diameters were averaged. Standard statistical formulae were used to calculate $\bar{d}$, the mean diameter, and σ, the variance on the mean, which here represents the spread of particle sizes.

3. RESULTS

A typical area of the "fresh" catalyst material following its initial reduction in flowing H_2 at 400°C for 3 hr is shown in Fig. 1. The method of specimen mounting for TEM is clearly evident with clustered alumina crystallites overlapping a hole in the carbon support film. The catalyst particles are best discerned from a "bird's eye" view and their small size is apparent by reference to the 0.46-nm (111) γ-Al_2O_3 lattice planes visible. The observation of such small particles is obviously highly dependent on both the microscope operating conditions and on the characteristics of the specimen (*3*). Competing contrast from the alumina support was especially strong in this study and 100% efficiency in particle detection could not always be verified. It was found, however, that particle diameters in the initial reduced catalysts, with Pt loadings, of 0.4–0.5 wt%, averaged around 1 nm. Moreover, mean diameters did not increase markedly for higher metal loadings although interparticle separations were reduced.

The statistical information relating to the catalysts and their various treatments is summarised in Tables 1 and 2.

3.1. Reforming Cycle

The low metal loading of Catalyst A, namely, 0.4% by weight of platinum, hampered the collection of good statistical data. The TEM diameters are therefore tabulated as approximate mean values only and serve more as a qualitative guide to the changes in the PSD.

TEM observations established that the reduced catalyst had a mean particle diameter of less than 1 nm and the resultant high Pt surface area was confirmed by hydrogen chemisorption uptake. The catalyst was then aged in a laboratory-scale naphtha reformer and it was found, on discharge, to contain 2.9% by weight of carbon deposit. The carbon was subsequently burnt off, via a controlled oxidation in flowing 3% by volume of O_2 in N_2. No significant increase in particle diameter after ageing or burnoff stages was found by TEM, despite the

FIG. 1. Region of the "fresh" platinum/alumina catalyst after initial reduction in flowing hydrogen at 400°C for 3 hr. The size of the Pt particles (some are arrowed) is indicated by comparison with the 0.46-nm (111) lattice fringes of γ-Al_2O_3.

TABLE 1

Reforming Cycle

Catalyst	Treatment	TEM diameter d (nm)	H_2 chemisorption V_m (ml/g)	$\bar{d}_{calc}$ (nm)
A (0.4 w/o Pt)	Reduced	<1	0.41	0.8
	Aged	~1.2		
	Burnt off	~1.4	0.22	1.5
	Oxychlorinated	~6.5		

change in the chemisorption capacity after burnoff. The burnt-off catalyst was then oxychlorinated to a chlorine loading of 1.71 wt%. TEM examination then indicated a mean particle diameter of around 6.5 nm.

Since the entire reforming cycle was carried out at no more than 500°C and the observed PSDs indicated increased sintering for oxidising treatment, in particular for the oxychlorination step, then further studies of other catalysts after more severe reducing and oxidising treatments were commenced. Furthermore, it was also decided that the TEM detection difficulties encountered with Catalyst A could be alleviated somewhat by using a $Pt/\gamma\text{-}Al_2O_3$ catalyst with higher metal loading.

3.2. Reducing Treatments

Heating Catalyst A at 600°C in flowing H_2 for 24 days resulted in only a small increase in mean particle diameter from less than 1 nm in the fresh catalyst to 1.6 ± 0.2 nm. Similar treatment of Catalyst B for 144 hr increased the particle diameter from 1.1 ± 0.4 nm for the fresh catalyst to 1.5 ± 0.9 nm. Comparable mean diameters, despite the shorter treatment time for B, resulted from the higher metal loading of Catalyst B. Figure 2 shows an area of Catalyst A after high-temperature reduction, again with the alumina overlapping a hole in the carbon support film, which clearly demonstrates the imaging of sub-2-nm-diameter particles on alumina. Figure 3 shows a region of Catalyst B following the high-temperature re-

TABLE 2

Treated Catalysts

Catalyst	Treatment	TEM diameter $\bar{d} \pm \sigma$ (nm)	H_2 chemisorption V_m (ml/g)	$\bar{d}_{calc}$ (nm)
A	H_2/600°C/24 days	1.6 ± 0.2	0.12	2.8
(0.4 w/o Pt)	3 v/o O_2 in N_2 600°C/24 days	20–200 (mean ~50)	0.13	2.5
B	Reduced	1.1 ± 0.4	1.45	1.1
(2.0 w/o Pt)	(i) H_2/600°C/144 hr	1.5 ± 0.9	0.66	2.5
	+ oxychlorination 500°C/4–6 hr	6.0 ± 2.6	1.04	1.6
B	Reduced	1.1 ± 0.4	1.45	1.1
(2.0 w/o Pt)	3 v/o O_2 in N_2 600°C/24 hr	21.0 ± 10.5	0.80	2.1
	+ (ii) 3 v/o O_2 in N_2 500°C/24 hr	18.0 ± 9.0	0.76	2.2
	+ oxychlorination 500°C/4–6 hr	25.0 ± 17.0	0.70	2.4

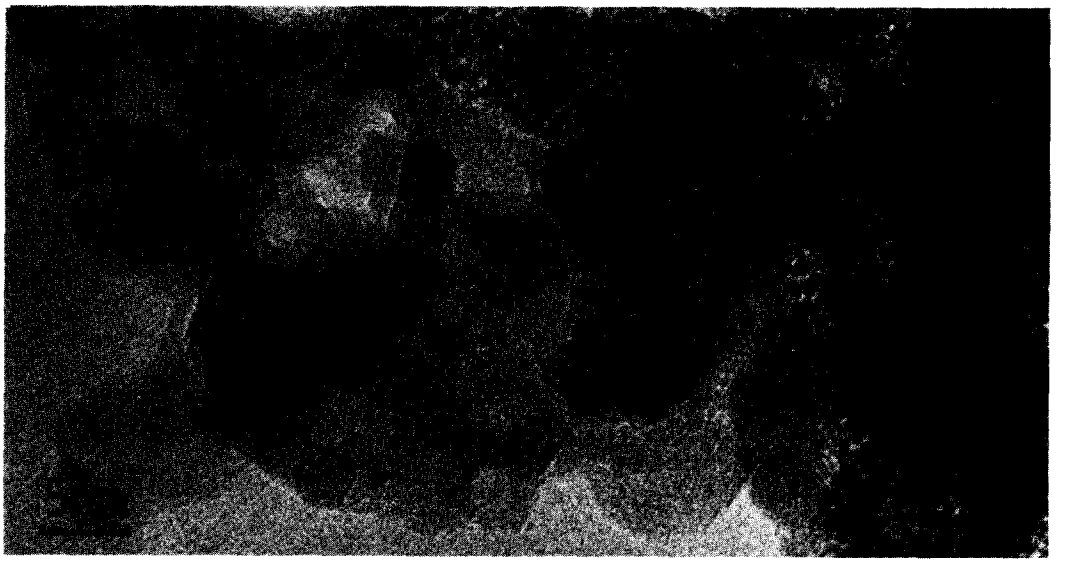

FIG. 2. Region of Catalyst A (0.4 w/o Pt) after reduction at 600°C for 24 days.

duction: the higher particle density is evident, several larger-diameter particles are imaged, and some shape resolution has been obtained.

The structure of these hydrogen-sintered particles (Cat. B) was subsequently examined at 500 kV in the HREM. Platinum 0.227-nm (111) and 0.196-nm (200) lattice fringes were well resolved and showed single crystal or twinned platinum particles (Figs. 4a and b, respectively). The γ-Al_2O_3 lattice structure was also often resolved, providing fringe contrast competing with the Pt particles, although higher scattering amplitude could normally distinguish the Pt particles from the support. Analysis of

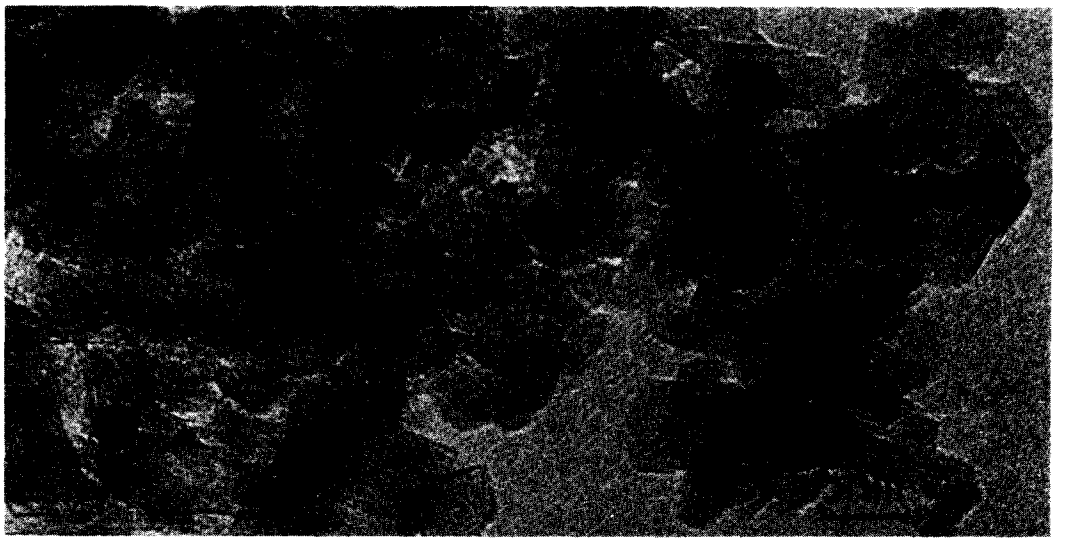

FIG. 3. Region of Catalyst B (2.0 w/o Pt) after reduction of 600°C for 144 hr. Larger particle size (cf. Fig. 2) is due to heavier Pt-loading.

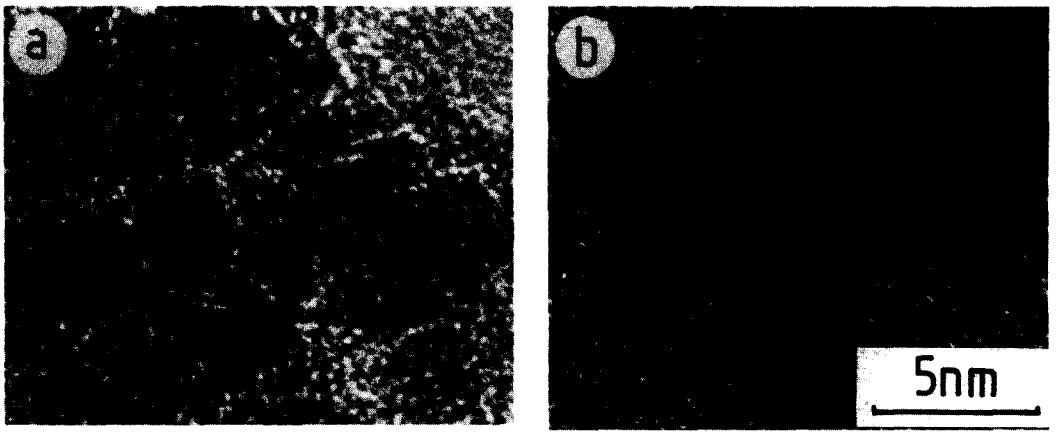

FIG. 4. High-resolution lattice images of Catalyst B (recorded at 500 kV). (a) Single crystal of Pt, (b) small lamellar-twinned particle of Pt. Note fringes from the γ-Al_2O_3 support.

high-resolution micrographs using the optical bench revealed only platinum and γ-Al_2O_3 periodicities. Figure 5 shows lattice fringes arising from several Pt crystallites, for example, at X and Y, and also a small region of γ-Al_2O_3 (arrowed) where the (100) projection of the unit cell is well resolved. It should be noted that mean particle diameters calculated from the hydrogen chemisorption measurements suggested larger particle diameters than those indicated by the TEM observations, even allowing for the severe approximations made of the particle geometry.

3.3. Oxidising Treatments

Heat treatment at 600°C in flowing 3% by volume of O_2 in N_2 was shown by TEM to lead to extensive particle agglomeration (see Fig. 6); a large increase in "mean" particle diameter was generally observed even after 24 hr, accompanied by considerable broadening of the PSD. Figure 7 provides a graphic comparison of the distributions for both reduced and oxidised samples from Catalyst B. Note, however, that chemisorptive losses for oxidised catalysts were relatively small in contrast to the extensive sintering observed by TEM.

It has been reported that redispersion occurs for platinum/alumina catalysts after oxidation at 600°C followed by further oxidation at 500°C (*12, 14*). Hence the high-temperature oxidation of Catalyst B was followed by reheating in 3 v/o O_2 in N_2 at 500°C for a further 24 hr. Whilst there was a small decrease in the overall mean particle diameter, the difference is hardly statistically significant. Moreover, no increase in chemisorptive capacity was measured. Subsequent reduction of an oxidised catalyst did not show any alterations in PSD. Our results thus do not provide confirmatory evidence of the redispersion behaviour previously reported.

3.4. Oxychlorinated Catalysts

Oxychlorination was carried out as part of the reforming cycle for Catalyst A and for two of the samples derived from Catalyst B, labelled (i) and (ii) in Table 2. Chlorine contents before and after treatment were found to be 0.17 w/o and 0.86 w/o for (i) and 0.50 w/o and 0.83 w/o for (ii). For each case the TEM observations indicated increased particle diameter after oxychlorination—see Tables 1 and 2. Many individual particles had irregular profiles (Fig. 8) and the alumina support structure was often visible through them. However, it is known that this does not necessarily indicate "raft-like" structure (*25*), so specimen-tilting experiments were conducted to determine the three-dimensional particle

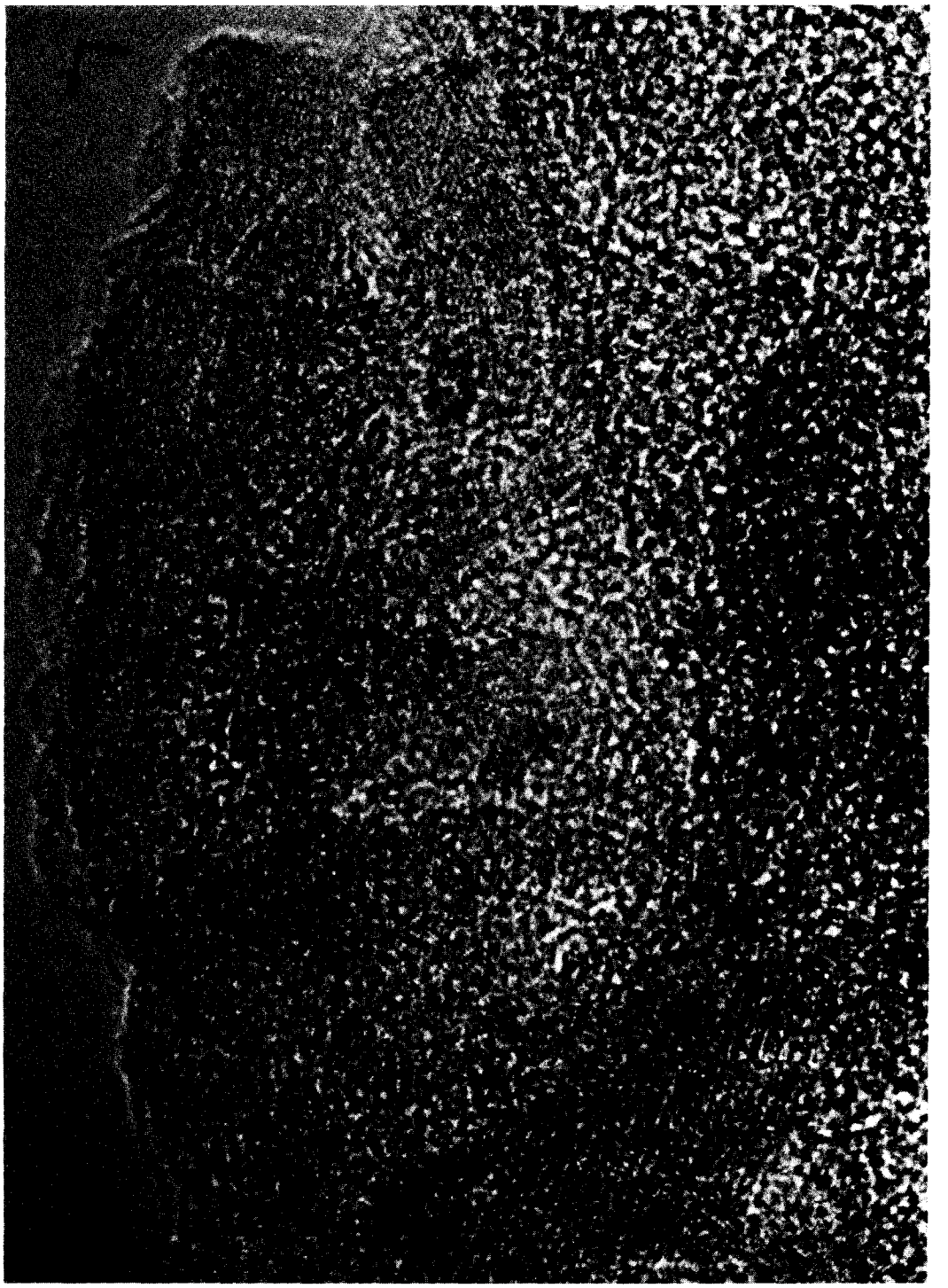

FIG. 5. Region of Catalyst B showing lattice fringes in several Pt particles (examples at X and Y) as well as the γ-Al_2O_3 support. A small region of (100) projection of γ-Al_2O_3 is indicated.

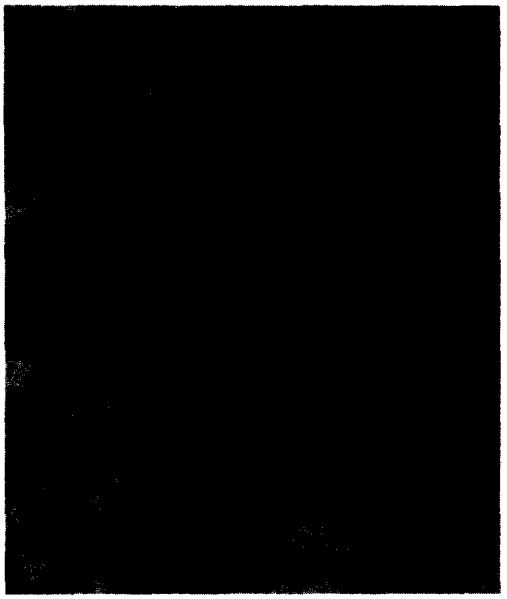

FIG. 6. Image demonstrating extensive particle agglomeration following oxidative treatment at 600°C.

geometry. Stereo images obtained with tilt angles differing by 5° showed that the sintered particles consisted of many smaller crystallites bonded randomly together and distributed irregularly throughout the alumina support. No evidence was found for actual gaps between the clustered crystallites, but re-entrant surfaces were observed. Electron diffraction and dark-field imaging indicated partial alignment of crystallites over some areas of the clusters, but large single crystals did not appear to be formed. Individual particles therefore maintained structural integrity but bonded together to form continuous, dendritic agglomerates, apparently confined only by the three-dimensional geometry of the porous alumina support. These irregular structural features, also seen in the simply oxidised specimen, though to a lesser degree, account for the high chemisorptive capacities of the oxidised and oxychlorinated catalysts (Table 2).

The crystalline nature of the sintered particles was again revealed by high-resolution lattice imaging. Figures 9a and b, for example, show regions of samples (i) and (ii), respectively, following oxychlorination. It was interesting that hydrogen chemisorption measurements for sample (i) indicated that it had regained platinum surface area after oxychlorination despite the considerable increase in particle diameter observed in the TEM. The chemisorption capacity of sample (ii), the oxidised catalyst, was reduced slightly by the oxychlorination treatment, but due to the irregular particle geometries no significant correlation could be properly made with the TEM diameter. Finally, it should be noted that there was no

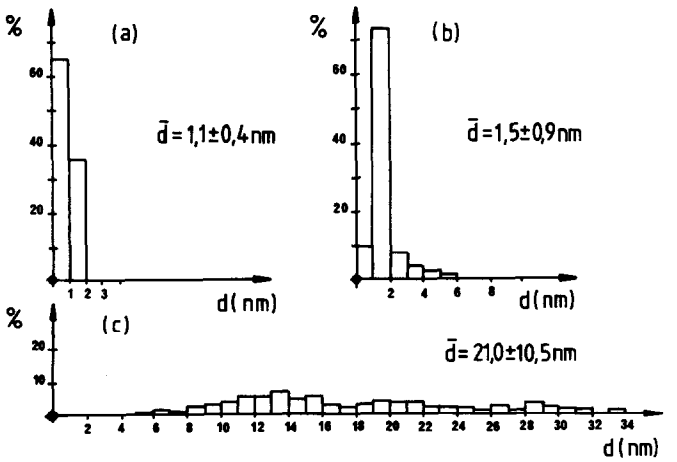

FIG. 7. Graphic representation of the changes in particle size distribution of Catalyst B following heat treatment. (a) "Fresh," (b) H_2/600°C/144 hr, (c) 3 v/o O_2 in N_2/600°C/24 hr.

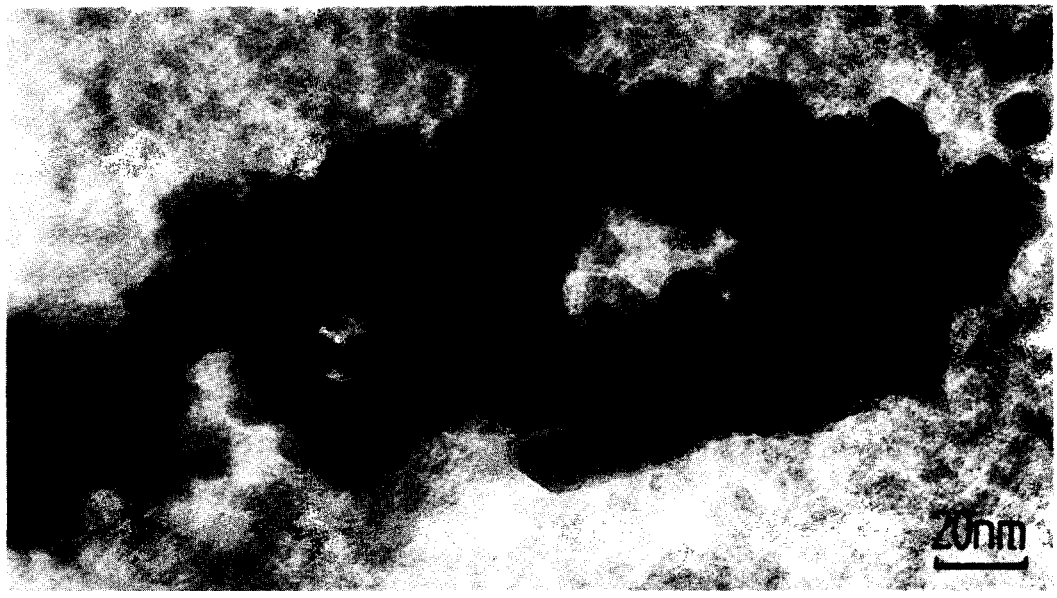

FIG. 8. Typical region of Catalyst B showing the particle agglomeration resulting from oxychlorination treatment at 600°C.

evidence, TEM or otherwise, for any oxides or oxychlorides of platinum.

4. DISCUSSION AND CONCLUSIONS

In a laboratory-scale reforming cycle, the oxidative step (oxychlorination) had the most marked effect on the catalyst (which consisted here of 0.4 w/o Pt · 0.8 w/o Cl γ-Al_2O_3). This procedure clearly increased the platinum mobility on the alumina support resulting in substantial sintering.

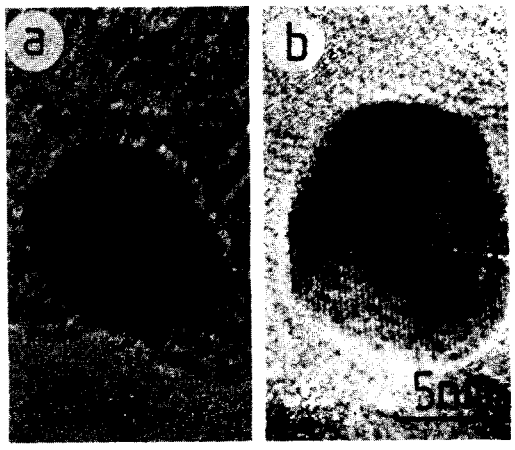

FIG. 9. Small crystalline particles of platinum after oxychlorination. (a) Sample (i), (b) sample (ii). (See Table 2 for more details.)

Further high-temperature treatments, in both reducing and oxidising environments, indicated the increased particle growth for the latter, as illustrated by the PSDs observed by TEM. However, it was significant that hydrogen chemisorption measurements showed that the Pt surface area losses were similar for both treatments, despite considerable differences in the PSDs and particle geometries indicated by TEM. Stereo-imaging of the oxidatively sintered particles revealed a highly irregular three-dimensional morphology, with dendritic agglomerates and many re-entrant surfaces, which would appear to account for the high chemisorptive capacities observed for these sintered catalysts. Dautzenberg and Wolters (*26*) have reported similar behaviour for their Pt/Al_2O_3 catalysts, in particular the formation, by agglomeration during high-temperature oxidising treatments, of large crystallites, which were not subsequently redispersed by 500°C oxidation. Note that all specimens had been exposed to air at room temperature so, presumably,

the Pt particles could have had a thin surface oxide layer; however, no bulk platinum oxides or oxychlorides were observed. Despite the overall marked variation in geometry, direct lattice resolution showed that the particles consisted, primarily at least, of platinum metal whether reducing or oxidising conditions had been employed; single crystals in particles down to 1.5 nm diameter, and twinned structures, were observed. Thus the catalytic activity of the metal component must arise from the various regular and defect structures on these crystal surfaces. This was also the conclusion of previous Low Energy Electron Diffraction (LEED) studies of Pt single-crystal surfaces (*27*).

The proposals for platinum re-dispersion by crystallite fracture (*14*) or by the oxide-spreading mechanism (*16*) seem to be unlikely from the present study. Indeed, it appeared that no accurate correlation was possible between hydrogen chemisorption value and PSD. It therefore seems probable, in the absence of a particle size effect, that "re-dispersion" for Pt/Al_2O_3 catalysts means the recovery of Pt sites which were lost to the chemisorption process. This is exemplified by Catalyst B after H_2/144 hr/600°C, followed by oxychlorination; the last step regained the chemisorption capacity, despite increased "mean" particle diameter. This possibility is further supported by Menon and Froment (*28*), who noted a loss in H_2 chemisorption capacity accompanied by reduced catalytic activity of Pt/Al_2O_3 catalysts after a 600°C/H_2 pretreatment. However, this loss could be reversed, and the catalytic activity restored, by a 500°C air oxidation and subsequent 400°C reduction.

This work has shown discrepancies in the correlation between particle size and shape and hydrogen chemisorption. In particular it has shown that simple *particle* re-dispersion is not an adequate explanation for recovery of catalytic activity. There was no evidence for particle breakup and the only possibility for physical re-dispersion is that crystal nuclei of less than 5 Å diameter separated from the main particle under the influence of the oxychlorinating atmosphere. This was below the discernible limit of the microscope and therefore this possibility, although energetically unlikely, remains. What is more feasible is that oxidising atmospheres reactivate surface sites on the particles that are responsible for catalytic activity. These sites also chemisorb hydrogen. Hence the correlation between catalytic activity and chemisorption, and the lack of agreement between these factors and the apparent physical dispersion of the platinum. Although a full catalytic profile was not obtained for these catalysts, they had shown reasonable catalytic activity when fresh and standard thermal treatments and gas atmospheres were used throughout. It is recognised that more extreme temperatures (e.g., >650°C) can cause extensive catalyst changes but these are beyond the scope of this work.

Finally, it should be recorded that recent experiments using this type of catalyst for reforming of *n*-heptane have shown that burnoff, followed by oxychlorination, of aged catalysts produces comparable catalytic activity to that of fresh catalysts, with similar PSD changes to those described here (*19*). The full catalytic results will be the subject of a future publication.

ACKNOWLEDGMENTS

The Cambridge University 600-kV high-resolution electron microscope was constructed as a joint project between the Cavendish Laboratory and the Department of Engineering with major financial support from the Science Research Council; continuing support from the Science and Engineering Research Council is gratefully acknowledged. One of us (D.W.) is grateful for a cooperative award from the S.R.C. and I.C.I. PLC Petrochemical and Plastics Division, Wilton.

REFERENCES

1. Zenith, J., Contreras L., J. L., Dominguez E., J. M., and Yacaman, M. J., *J. Microsc. Spectrosc. Electron.* **5**, 291 (1980).
2. Sprys, J. W., Bartosiewicz, L., McCune, R. and Plummer, H. K., *J. Catal.* **39**, 91 (1975).

3. Flynn, P. C., Wanke, S. E., and Turner, P. S., *J. Catal.* **33,** 233 (1974).
4. White, D., Baird, T., Fryer, J., and Smith, D. J., *in* "Electron Microscopy and Analysis 1981" (M. J. Goringe, Ed.), p. 403. Institute of Physics, Bristol, 1982.
5. Baker, R. T. K., Prestridge, E. B., and Garten, R. L., *J. Catal.* **56,** 390 (1979).
6. Chu, Y. F., and Ruckenstein, E., *J. Catal.* **55,** 281 (1978).
7. Chen, M., and Schmidt, L. D., *J. Catal.* **55,** 348 (1978).
8. White, D., Baird, T., and Fryer, J. R., *in* "Electron Microscopy 1980" (P. Brederoo and G. van Boom, Eds.), Vol. 1, p. 220. Seventh European Regional Conference on Electron Microscopy Foundation, Leiden, 1980.
9. Smith, D. J., White, D., Baird, T., and Fryer, J. R., *J. Catal.* **81,** 107 (1983).
10. Glassl, H., Kramer, R., and Hayek, K., *J. Catal.* **63,** 167 (1980).
11. Spenadel, L., and Boudart, M., *J. Phys. Chem.* **64,** 204 (1960).
12. Straguzzi, G. I., Aduriz, H. R., and Gigola, C. E., *J. Catal.* **66,** 171 (1980).
13. Yao, H. C., Sieg, M., and Plummer, H. K., *J. Catal.* **59,** 365 (1979).
14. Ruckenstein, E., and Malhotra, M. L., *J. Catal.* **41,** 303 (1976).
15. Stulga, J. E., Wynblatt, O., and Tien, J. K., *J. Catal.* **62,** 59 (1980).
16. Ruckenstein, E., and Chu, Y. F., *J. Catal.* **59,** 109 (1979).
17. Baker, R. T. K., *J. Catal.* **63,** 523 (1980).
18. Wang, T., and Schmidt, L. D., *J. Catal.* **70,** 187 (1981).
19. Foger, K., and Jaeger, H., *J. Catal.* **70,** 53 (1981).
20. Derouane, E. G., Baker, R. T. K., Dumesic, J. A., and Sherwood, R. D., *J. Catal.* **69,** 101 (1981).
21. McHenry, K. W., Bertolacini, R. J., Brennan, H. M., Wilson, J. L., and Seelig, H. S., *in* "Actes du Deuxième Congrès Internationale de Catalyse (Paris, 1960)," Vol. 2, p. 2295. Technip, Paris, 1961.
22. Nixon, W. C., Ahmed, H., Catto, C. J. D., Cleaver, J. R. A., Smith, K. C. A., Timbs, A. E., Turner, P. W., and Ross, P. M., *in* "Developments in Electron Microscopy and Analysis 1977" (D. L. Misell, Ed.), p. 13. Institute of Physics, Bristol, 1978.
23. Cosslett, V. E., *Proc. Roy. Soc. (London) Sect. A* **370,** 1 (1980).
24. Smith, D. J., and Marks, L. D., *Philos. Mag. A* **44,** 735 (1981).
25. Treacy, M. M. J., and Howie, A., *J. Catal.* **63,** 265 (1980).
26. Dautzenberg, F. M., and Wolters, H. B. M., *J. Catal.* **51,** 26 (1978).
27. Somorjai, G. A., *Advan. Catal.* **26,** 1 (1977).
28. Menon, P. G., and Froment, G. F., *J. Catal.* **59,** 138 (1979).
29. Spanner, M., private communication.